



Sintering-modified mixed Ni–Co–Cu oxymanganospinel for NTC electroceramics

O. Shpotyuk^{a,b,*}, V. Balitska^{a,c}, I. Hadzaman^a, H. Klym^a

^a Lviv Scientific Research Institute of Materials of SRC “Carat”, 202 Stryjska Str., Lviv, UA 79031, Ukraine

^b Institute of Physics of Jan Długosz University, 13/15, al. Armii Krajowej, Częstochowa, PL 42201, Poland

^c Lviv State University of Vital Activity Safety, 35, Kleparivska Str., Lviv, 79007, Ukraine

ARTICLE INFO

Article history:

Received 4 June 2010

Accepted 14 September 2010

Available online 12 October 2010

Keywords:

Sintering

Ceramics

Disordered systems

Sintering

Scanning electron microscopy

ABSTRACT

Mixed Ni–Co–Cu oxymanganospinel of $\text{Cu}_{0.1}\text{Ni}_{0.8}\text{Co}_{0.2}\text{Mn}_{1.9}\text{O}_4$ composition with improved functional reliability are first developed for possible application as high-precise NTC thermistors. It is established the amount of additional rock-salt NiO phase in these ceramics, which was not externally introduced at the initial stages of ceramics processing, but extracted during sintering route occurs a decisive role to inhibit the parasitic degradation caused by thermal storage at the elevated temperatures. This effect is well revealed only in ceramics having a character fine-grain microstructure obtained due to injection of small amount of thermally transferred energy, while structural monolithization caused by great value of thermally transferred energy into ceramics bulk reveals an opposite influence. The fact, the ceramics with fine-grain microstructure and large content of rock-salt NiO extractions demonstrate the best suitability for stretched-exponential relaxation kinetics (the most appropriate one for describing degradation kinetics in structurally dispersive solids like ceramics) serves as additional confirmation to the above conclusion.

© 2010 Elsevier B.V. All rights reserved.

1. Introduction

Oxymanganospinel $\text{Cu}_{0.1}\text{Ni}_{0.8}\text{Co}_{0.2}\text{Mn}_{1.9}\text{O}_4$ ceramics are one of the most perspective materials for device application as negative temperature coefficient (NTC) thermistors, precise temperature measuring systems and sensors, in-rush current limiters [1,2]. That is why the problem of their functional stability and reliability is of high importance.

As a rule, to eliminate parasitic influence of degradation effects in NTC electroceramics, the methods of their chemical modification by metallic additives at the initial stages of technological preparation have been usually used [3,4]. These metallic additives, being located near inter-granular regions in the vicinity of grain boundaries, diminish thermally activated ageing phenomena by stabilizing intrinsic cationic distribution within individual ceramics grains. As a result, the chemically modified ceramics typically show a higher stability in comparison with non-modified ones.

A principally different approach alternative to the above one is developed in this work. In part, the additional rock-salt phase, which was not externally introduced at the initial stages of ceramics

processing, but only segregated during high-temperature sintering serves as an effective barrier to inhibit further degradation in spinel-type $\text{Cu}_{0.1}\text{Ni}_{0.8}\text{Co}_{0.2}\text{Mn}_{1.9}\text{O}_4$ ceramics.

2. Materials and methods

Precise amounts of high-purity and previously tested carbonate salts corresponding to the final $\text{Cu}_{0.1}\text{Ni}_{0.8}\text{Co}_{0.2}\text{Mn}_{1.9}\text{O}_4$ composition were weighed and wet mixed. The mixture was thermally decomposed in the air at $700 \pm 5^\circ\text{C}$ for 4 h. Then, the obtained powders were milled, blended with organic binder and pressed into disks of approximately 10 mm in diameter and 1 mm in thickness.

The prepared blanks were sintered in the air at different temperatures of T_s being 1040, 1200 and 1300°C . The sintering route was arranged in such a way to ensure the necessary conditions for inhibition effect in degradation [5], the content of additionally extracted NiO phase with rock-salt NaCl-type structure having a decisive role. In fact, we deal with Ni-deficient ceramics in respect to stoichiometric $\text{Cu}_{0.1}\text{Ni}_{0.8}\text{Co}_{0.2}\text{Mn}_{1.9}\text{O}_4$ composition taken as a starting one in disproportionality calculations.

Four batches of ceramics with 1–12% of NiO extractions were prepared according to the regimes presented in Table 1. These regimes correspond to different portions of thermal energy transferred into ceramics during sintering. The latter was numerically determined as a square restricted by temperature–time curves above horizontal line corresponding to 920°C , the temperature of monophasic $\text{Cu}_{0.1}\text{Ni}_{0.8}\text{Co}_{0.2}\text{Mn}_{1.9}\text{O}_4$ ceramics formation [6] (Fig. 1).

To study the microstructure of ceramics, the X-ray diffraction (XRD) patterns were recorded at room temperature using HZG-4a powder diffractometer with $\text{CuK}\alpha$ and/or $\text{FeK}\alpha$ radiation. The measurements were carried out in $2\theta = 0.02\text{--}0.05^\circ$ diffraction angle steps with a variable scanning rate depending on the sample quality. The profile analysis of XRD patterns was performed using pseudo-Voigt profile function. The lattice parameters and crystal structure of all phases presented in the samples under consideration were determined using the Rietveld methods with

* Corresponding author at: Lviv Scientific Research Institute of Materials of SRC “Carat”, 202 Stryjska Str., Lviv, UA 79031, Ukraine.

Tel.: +380 0322 63 83 03; fax: +380 0322 949733.

E-mail address: shpotyuk@novas.lviv.ua (O. Shpotyuk).

Table 1
Technological regimes of $\text{Cu}_{0.1}\text{Ni}_{0.8}\text{Co}_{0.2}\text{Mn}_{1.9}\text{O}_4$ ceramics preparation.

Batch No. 1		Batch No. 2		Batch No. 3		Batch No. 4	
<i>t</i> (min)	<i>T</i> (°C)	<i>t</i> (min)	<i>T</i> (°C)	<i>t</i> (min)	<i>T</i> (°C)	<i>t</i> (min)	<i>T</i> (°C)
350	600	350	600	350	600	350	600
493	1040	545	1200	545	1200	578	1300
673	1040	605	1200	605	1200	638	1300
1015	850	1235	850	815	850	908	850
1115	25	1295	100	875	100	1015	25
		1350	100	925	25		

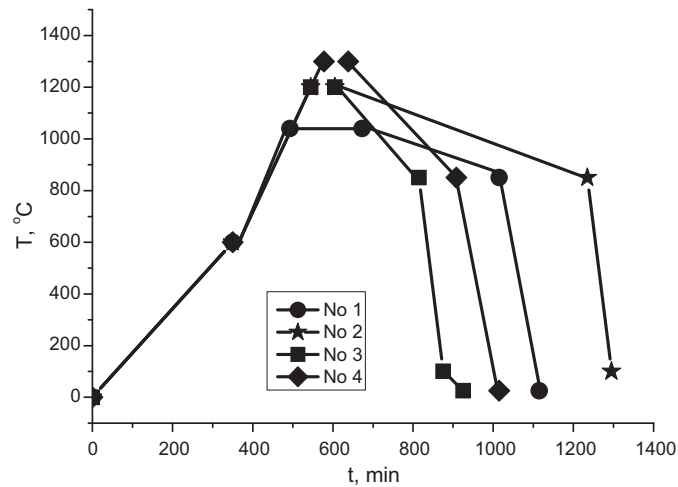


Fig. 1. Temperature–time curves corresponding to different technological regimes of $\text{Cu}_{0.1}\text{Ni}_{0.8}\text{Co}_{0.2}\text{Mn}_{1.9}\text{O}_4$ ceramics preparation.

WinCSD [7] and FULLPROF.2k from WinPLOTR programs software [8]. The values of thermally transferred energy and amount of NiO phase in the studied ceramics estimated with XRD are presented in Table 2.

The morphological structure of ceramics was probed using electron microscope JSM-6700F (Japan), cross-sections morphology being tested near surface (0–70 μm depth) and chip centres.

Electrical resistance measurements were performed with digital multimeter. The results of ageing tests were controlled by relative resistance drift (RRD) $\Delta R/R_0$ caused by ceramics storage at the temperature of 170 °C. These measurements were carried out in the normal conditions at 25 °C after certain hours of thermal exposure (24, 72, 144, 288 and 500 h). The confidence interval in RRD measuring bar restricted by equipment accuracy was no more than 0.2%. Possible deviations in some experimental points were caused by additional faults in exact reproduction of degradation cycles conditions (cooling regime from the temperature of ageing tests down to the temperature of electrical measurements, influence of environment atmosphere and humidity, etc.). The performed statistical analysis testified that the above factors introduced only additional fault about $\pm 0.2\%$ in the measured $\Delta R/R_0$ values. So, the maximal overall error of electrical measurements did not exceed approximately $\pm 0.5\%$.

With a purpose of adequate mathematical description of the observed degradation kinetics, the numerical values of different fitting parameters in the typical relaxation functions (RF) were calculated in such a way to minimize the mean-square deviation *err* of experimentally measured points from chosen RF possible as adequate solution of general degradation Eq. (1) [9]:

$$\frac{d\eta}{dt} = -\lambda\eta^\alpha t^\beta, \quad (1)$$

where power indexes α and β as well as λ coefficient are some material-related constants.

Table 2
Thermal energies transferred during sintering into $\text{Cu}_{0.1}\text{Ni}_{0.8}\text{Co}_{0.2}\text{Mn}_{1.9}\text{O}_4$ ceramics.

Ceramics batch No.	Thermally transferred energy		Maximal <i>T_s</i> °C	NiO content %
	°C min	a.u.		
1	175	1.0	1040	1
2	465	2.7	1200	10
3	190	1.1	1200	12
4	465	2.7	1300	12

As it was first pointed out in [9,10], there are 5 typical RF as possible solutions of the above differential Eq. (1) in dependence on α and β values.

If $\alpha = 1$ and $\beta = 0$, the simple exponential monomolecular RF 1 proper for activation processes determined by one prevailing value of activation energy into more equilibration state (the similar processes can be observed, as a rule, in crystalline solids) is a solution of Eq. (2):

$$\eta(t) = \exp\left(\frac{-t}{\tau}\right), \quad (2)$$

where $\tau = 1/\lambda$, $\lambda \neq 0$.

If degradation is caused by recombination of specific structural defects of opposite nature, such as electrons and holes, interstitials and vacancies, their degradation is determined by bimolecular RF 2, which corresponds to $\alpha = 2$ and $\beta = 0$ in Eq. (3):

$$\eta(t) = \left(1 + \frac{t}{\tau}\right)^{-1}, \quad (3)$$

where $\tau = 1/\lambda$, $\lambda \neq 0$.

The strict solution of Eq. (1) at $\alpha \neq 0$ and $\beta = 0$ can be presented in the form of a so-called partly generalized RF 3, this function being often used for description of thermally induced effects in some oxide glasses:

$$\eta(t) = \left(1 + \frac{t}{\tau}\right)^{-\kappa}, \quad (4)$$

where $\tau = 1/[\lambda(\alpha - 1)]$, $\kappa = 1/(\alpha - 1)$, $\alpha \neq 1$, $\lambda \neq 0$.

In the case of $\alpha = 1$ and $\beta \neq 0$, the degradation kinetics is defined by stretched-exponential RF 4, the most adequate mathematical function for relaxation in a large number of disordered solids:

$$\eta(t) = \exp\left[\left(\frac{-t}{\tau}\right)^\kappa\right], \quad (5)$$

where $\tau = (1 + \beta)/\lambda$, $\kappa = 1 + \beta$, $\beta \neq -1$, $\lambda \neq 0$.

The exact general solution of Eq. (1) is given by fully generalized RF 5 ($\alpha \neq 0$, $\beta \neq 0$):

$$\eta(t) = \left[\left(1 + \frac{t}{\tau}\right)^{-\kappa}\right]^{-r}, \quad (6)$$

where $\tau = [(1 + \beta)/\lambda(\alpha - 1)]^{1/(1 + \beta)}$, $\kappa = 1 + \beta$, $r = 1/(\alpha - 1)$, $\alpha \neq 1$, $\beta \neq -1$, $\lambda \neq 0$.

The most suitable RF for the observed degradation kinetics was chosen at the basis of comparison of the calculated *err* values, taking into account also the overall number of fitting parameters.

3. Results and discussion

The degradation of $(\text{Cu,Ni,Co,Mn})_3\text{O}_4$ mixed transition-metal manganite ceramics is known to be mainly governed by thermally stimulated exchange in the occupation of tetra- and octahedral sites within spinel-structured grains by transition-metal cations preferentially such as Mn^{3+} and Mn^{4+} [5,6]. These cation redistribution processes can be effectively blocked by additional rock-salt phase extracted at the intergranular boundaries between ceramics grains [5]. So it is expected the more content of this extracted phase, the high stability of the prepared ceramics will be achieved. Being within above assumption, we tried to choose the spinel-type $\text{Cu}_{0.1}\text{Ni}_{0.8}\text{Co}_{0.2}\text{Mn}_{1.9}\text{O}_4$ ceramics with optimal amount of additional NiO rock-salt phase served as a barrier to inhibit cation-redistribution degradation. The sintering route (the maximal temperature of sintering and cooling rate) was arranged in such a way to prepare ceramics of principally different microstructural morphology. This allows to clear conditions necessary to inhibit degradation processes in the $\text{Cu}_{0.1}\text{Ni}_{0.8}\text{Co}_{0.2}\text{Mn}_{1.9}\text{O}_4$ ceramics.

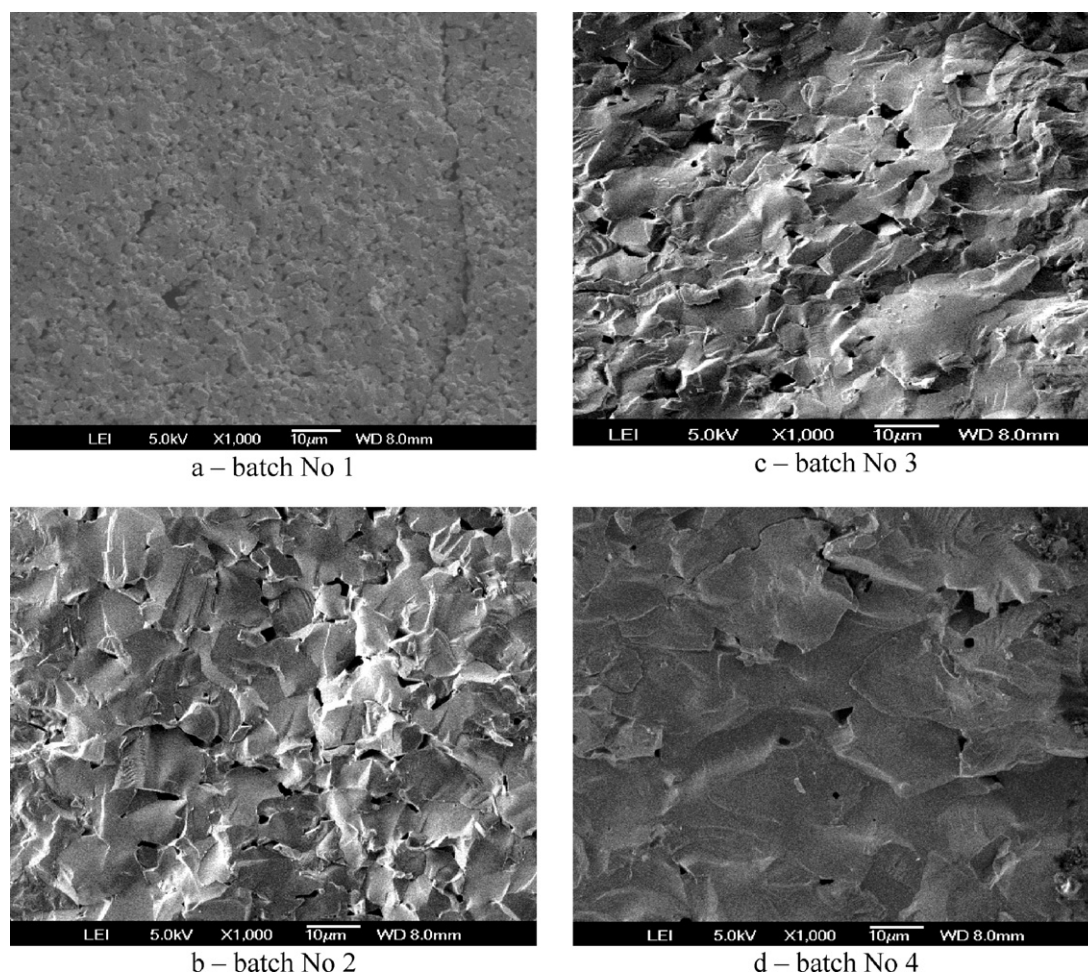


Fig. 2. Morphological structure of $\text{Cu}_{0.1}\text{Ni}_{0.8}\text{Co}_{0.2}\text{Mn}_{1.9}\text{O}_4$ ceramics.

As can be seen from Table 1, the first No. 1 batch of ceramics was prepared at relatively low temperature (1040°C) and cooling rate (33.3°C/h). The amount of thermal energy transferred into ceramics and additional NiO phase extracted within this process were, correspondingly, 175°C min and 1%. The second No. 2 batch of ceramics was sintered with the same rate of cooling, but at a more high sintering temperature (1200°C). Therefore, the thermally transferred energy was high too (at the level of 465°C min) and content of additional NiO phase reached 10%. The third No. 3 batch of ceramics was sintered at the same temperature (1200°C), but cooling rate was increased to 100°C/h . Correspondingly, the amount of thermal energy transferred into ceramics was decreased to about 90°C min , while the content of additional NiO phase reached 12%. Finally, the last No. 4 batch of ceramics was sintered at the highest temperature (1300°C), but at the same cooling rate (100°C/h). The amount of thermally transferred energy was as high as in the second case (465°C min), while the content of NiO phase was 12%.

The results of our electrical measurements testify that extractions of additional NiO phase in $\text{Cu}_{0.1}\text{Ni}_{0.8}\text{Co}_{0.2}\text{Mn}_{1.9}\text{O}_4$ ceramics alone are not necessary to effectively block the degradation processes. Indeed, despite activation energies of electrical conductivity for all ceramics batches do not change significantly, being at the level of $0.29\text{--}0.30\text{ eV}$, the values of their electrical conductivity at 25°C increases non-monotonically from 0.17 to $0.36\ \Omega^{-1}\text{ m}^{-1}$ for samples of No. 1, No. 3 and No. 2 batches, but drops down to $0.21\ \Omega^{-1}\text{ m}^{-1}$ for No. 4 batch samples (see Table 3). The above anomalous behavior is a character also for RRD caused by 170°C storage. The extremely small value of RRD near 2.5% is character

for samples of No. 3 batch (sintered at 1200°C) having 12% of additional NiO phase, while ceramics samples of batch No. 4 having the same amount of NiO phase but sintered at higher temperature (1300°C) demonstrate sharp increase in RRD up to 18%.

To explain this anomaly, the morphological structure of the prepared ceramics was carefully checked. As it follows from Fig. 2, the prepared ceramics differ significantly by evolution of their grain-pore microstructure. The batch No. 1 samples (Fig. 2a) are characterized by fine $1\text{--}3\ \mu\text{m}$ grains. The numerous intergranular pores are small enough, their sizes not exceeding $1\text{--}2\ \mu\text{m}$. White film, which can be attributed to additional rock-salt NiO phase extractions, weakly appears in these ceramics mainly near intergranular boundaries, sometimes it partially fills of pores. The samples of batch No. 2 (Fig. 2b) are characterized by larger grains with character sizes near $5\text{--}7\ \mu\text{m}$, some of them achieving $10\ \mu\text{m}$. White NiO film appears in these ceramics only in the regions of intergranular boundaries. The grain structure of the samples of batch No. 3 (Fig. 2c) is gradually different. The corresponding chip

Table 3
Electrical properties of $\text{Cu}_{0.1}\text{Ni}_{0.8}\text{Co}_{0.2}\text{Mn}_{1.9}\text{O}_4$ ceramics.

Ceramics batch No.	Conductivity σ (at 25°C) ($\Omega\text{ m}^{-1}$)	Activation energy E_a (eV)	$\Delta R/R_0$ (%)
1	0.17	0.30	30.0
2	0.36	0.29	3.5
3	0.27	0.29	2.5
4	0.21	0.30	18

Table 4Fitting parameters of different RF describing degradation kinetics in $\text{Cu}_{0.1}\text{Ni}_{0.8}\text{Co}_{0.2}\text{Mn}_{1.9}\text{O}_4$ ceramics.

Sample batch No.	Fitting parameters of RFs													
	RF 1, Eq. (2)		RF 2, Eq. (3)		RF 3, Eq. (4)			RF 4, Eq. (5)			RF 5, Eq. (6)			
	err	τ	err	τ	err	τ	κ	err	τ	κ	err	τ	κ	r
1	1.48	9.8	0.75	3.3	0.35	0.02	0.20	0.34	5.1	0.10	0.50	0.1	0.24	0.49
2	0.03	90.8	0.01	81.1	0.01	19.3	0.14	0.01	139.8	0.66	0.02	744.7	0.70	3.35
3	0.04	63.5	0.02	48.2	0.01	4.4	0.02	0.01	189.2	0.46	0.02	53.0	0.5	0.27
4	1.87	40.5	0.47	28.5	0.21	4.3	0.19	0.23	65.5	0.45	0.33	30.8	0.61	0.50

structure of these ceramics is more monolithic, it being characterized only by separate pores with 1–3 μm in sizes. White NiO film appears as bright layer of approximately 10 μm in thickness on the grain surface of these samples. In contrast, the grain structure of the samples of batch No. 4 (Fig. 2d) attains a fully monolithic shape. Only some individual pores of relatively large sizes (near 3–5 μm) are observed in these ceramics, the NiO phase extractions appearing as uniform layer on the whole ceramics surface.

Thus, the results of morphological study show that ceramics microstructure changes from fine-grained to monolithic one with corresponding increase in thermal energy transferred into ceramics bulk during sintering. This monolithization occurs as an inhibition influence on the degradation owing to NiO phase extractions. As a result, the samples of No. 4 batch having as high as 12% of NiO phase reveal a relatively sharp increase in RRD achieving as high as 18% (see Table 2).

The results of degradation kinetics modeling for $\text{Cu}_{0.1}\text{Ni}_{0.8}\text{Co}_{0.2}\text{Mn}_{1.9}\text{O}_4$ ceramics, presented in Table 4, give an additional confirmation for the above conclusion. The fitting of experimentally observed degradation kinetics by stretched-exponential RF 4 is shown to be most optimal in terms of mean-square deviations (the smallest *err* values in comparison with other RF whichever ceramics batch). The more dispersive ceramics (owing to extracted NiO inclusions and ceramics fine-grained structure), the better correspondence between RF 4 and experimental degradation kinetics (the cases of batches No. 2 and 3 ceramics samples). It should be noted that fitting route with partially generalized RF 3 gives also a quite good correspondence, but this function is not optimal one in view of large number of fitting parameters (3 versus 2 in RF 4).

It is quite understandable that extraction of additional NiO phase from spinel-structured $\text{Cu}_{0.1}\text{Ni}_{0.8}\text{Co}_{0.2}\text{Mn}_{1.9}\text{O}_4$ ceramics enlarges the dispersivity of the system, while the monolithization of ceramics structure causes an opposite effect. As a result, the ceramics samples of batch No. 3 demonstrate the best suitability for stretched-exponential RF 4 relaxation kinetics. That is why the non-exponentiality index *L* grows from 0.10 (batch No. 1) to 0.66 for batch No. 2 ceramics having a large amount of NiO, the similar increase being character for time constant τ too. However, the further increase in NiO content from 10 (batch No. 2) to 12% (batches No. 3 and 4) is associated with principally different processes of

microstructural evolution. As can be seen from Fig. 2, the batch No. 3 ceramics has a more fine-grained structure, while those, the batch No. 4, is more monolithized one. Therefore, despite nearly the same value of non-exponentiality index $L \approx 0.45$ –0.46, the time-constant τ increase from 139.8 to 189.2 h for ceramics batch No. 3 and to 65.5 h for ceramics batch No. 4 samples.

4. Conclusions

The spinel-structured mixed transition-metal manganite $\text{Cu}_{0.1}\text{Ni}_{0.8}\text{Co}_{0.2}\text{Mn}_{1.9}\text{O}_4$ ceramics with improved functional stability and reliability can be prepared within modified sintering technological route owing to optimal combination in the amount of additionally extracted rock-salt NiO phase and inner monolithization of the ceramics structure.

Acknowledgment

The authors acknowledge support from Science and Technology Center in Ukraine under regular STCU Project No 4277.

References

- [1] I.T. Sheftel, Thermoresistors, Nauka, Moscow, 1973.
- [2] J.A. Bekker, C.B. Green, G.L. Pearson, Trans. Am. Inst. Elect. Eng. 65 (1994) 711–725.
- [3] R. Metz, M. Brieu, R. Legros, A. Rousset, Colloque de Physique 51 (1990) 1003–1008.
- [4] P. Castelan, A. Bui, A. Loubiere, A. Rousset, R. Legros, Sens. Actuators A 33 (1992) 119–122.
- [5] O. Bodak, L. Akselrud, P. Demchenko, B. Kotur, O. Mrooz, I. Hadzaman, O. Shpotyuk, F. Aldinger, H. Seifert, S. Volkov, V. Pekhnyo, J. Alloys Compd. 347 (2002) 14–23.
- [6] I.V. Hadzaman, A.P. Kovalsky, O.Ya. Mrooz, O.I. Shpotyuk, Mater. Lett. 29 (1996) 195–198.
- [7] L. Akselrud, Yu. Grin, V. Pecharsky, P. Zavalij, B. Baumgariner, E. Wolfer, Use the CSD program package for structure determination from powder data, in: Proceedings of the Second European Powder Diffraction Conference (EPDIC), Enschede, The Netherlands, Trans. Tech. Pub. Pt 1, 1993, pp. 335–340.
- [8] T. Roisnel, J. Rodriguez-Carvajal, WinPLOT: a Windows tool for powder diffraction patterns analysis, in: R. Delhez, E.J. Mittenmeijer (Eds.), Proceeding of the Seventh European Powder Diffraction Conference (EPDIC 7), 2000, pp. 118–123.
- [9] V.O. Balitska, B. Butkiewicz, O.I. Shpotyuk, M.M. Vakiv, Microelectron. Reliab. 42 (2002) 2003–2007.
- [10] V.O. Balitska, M.M. Vakiv, O.I. Shpotyuk, B. Butkiewicz, L.I. Shpotyuk, J. Eur. Ceram. Soc. 24 (2004) 1243–1246.